

**Fermi National Accelerator Laboratory**

**FERMILAB-Conf-93/396-E**

**DØ**

## **Measurement of the W Mass in the DØ Detector**

**Presented by Qiang Zhu  
For the DØ Collaboration**

*Fermi National Accelerator Laboratory  
P.O. Box 500, Batavia, Illinois 60510*

*New York University, Department of Physics  
4 Washington Place, New York, New York 10003*

**December 1993**

**Presented at the 9th Topical Workshop on Proton-Antiproton Collider Physics,  
Tsukuba, Japan, October 18-22, 1993**

## **Disclaimer**

*This report was prepared as an account of work sponsored by an agency of the United States Government. Neither the United States Government nor any agency thereof, nor any of their employees, makes any warranty, express or implied, or assumes any legal liability or responsibility for the accuracy, completeness, or usefulness of any information, apparatus, product, or process disclosed, or represents that its use would not infringe privately owned rights. Reference herein to any specific commercial product, process, or service by trade name, trademark, manufacturer, or otherwise, does not necessarily constitute or imply its endorsement, recommendation, or favoring by the United States Government or any agency thereof. The views and opinions of authors expressed herein do not necessarily state or reflect those of the United States Government or any agency thereof.*

# Measurement of the W Mass in the DØ Detector

The DØ Collaboration

presented by Qiang Zhu

Department of Physics, New York University  
4 Washington Place, New York, N.Y. 10003, U.S.A.

We report the results of a preliminary analysis of the  $W \rightarrow e\nu$  decays observed in  $14 \text{ pb}^{-1}$  of data taken during the Fermilab Tevatron Run 1(a). After normalizing the mass scale to the Z mass measured at LEP, we find a value for the W mass of  $79.86 \pm 0.16(\text{stat}) \pm 0.20(\text{syst}) \pm 0.31(\text{scale}) \text{ GeV}$ . The method for extracting the W mass and the details of the error analysis are presented and discussed.

## 1. Introduction

The impressive successes of the  $SU(3)_c \times SU(2)_L \times U(1)$  gauge theory of strong and electroweak interactions have earned it the title “Standard Model.” It predicted the existence of  $W^\pm$  and  $Z^0$  bosons. Their discovery at CERN 10 years ago with close to the theoretically expected masses lent enormous support to the Model. The Z mass has been measured since with great precision at LEP,  $M_Z = 91.187 \pm 0.007 \text{ GeV}$ [1]. A precision measurement of the W mass, one of the parameters of the standard model, is needed.

The top quark is predicted by the Standard Model, but has yet to be observed. A precision measurement of the W mass combined with existing electroweak measurements would result in a tight constraint on the top quark mass[2].

Although the Standard Model has been very successful, it has its shortcomings. The  $SU(2)_L \times U(1)$  electroweak sector has a minimum of seventeen independent masses and couplings and its symmetry breaking is based on the trivial free field ( $\lambda\Phi^4$ ) theory. So there is reason for anticipating new physics. It will be interesting to see if the Standard Model holds up under improved electroweak measurements. Any deviation could be a hint of new physics[3, 4].

We describe here the measurement of the W mass in the DØ detector at the Tevatron. We discuss the triggers, offline event selection, and method used to set the electromagnetic energy scale. We make a detailed comparison between the data and a fast Monte Carlo simulation, and conclude with a discussion of various systematic errors, including the uncertainty from the energy scale. Some consistency checks are also performed.

## 2. Trigger and Offline Event Selection

The typical interaction rate at the Tevatron is  $\sim 10^5 \text{ Hz}$ . Two levels of triggers are employed to reduce this rate to an acceptable level for data logging. The Level 1 trigger is implemented in hardware and capable of making a decision in the time interval between two beam crossings, i.e. in  $3.5 \mu\text{s}$ . The output rate is about 100Hz. The Level 2 trigger relies on software event filters that run on a farm of 50 VAXstations. Events are processed in parallel

<i>W event kinematic cuts</i>	<i>Z event kinematic cuts</i>
one electron with $P_T > 25 \text{ GeV}$	two electrons
Missing $P_T > 25 \text{ GeV}$	each with
$P_T^W < 30 \text{ GeV}$	$P_T > 25 \text{ GeV}$

Table 1: W, Z event kinematic cuts

<i>W sample</i>			<i>Z sample</i>				
ECN	CC	ECS	ECN-ECN	ECN-CC	CC-CC	CC-ECS	ECS-ECS
1522	5830	1420	34	110	313	118	28

Table 2: W and Z samples

on the farm, each workstation processing one event a time. The output data is recorded on tape at a rate of 1 – 2 Hz for offline analysis.

The Level 1 trigger requires one EM tower with  $P_T$  above 10 GeV for W's, and two EM trigger towers each with  $P_T$  above 7 GeV for Z's. The size of the trigger tower is  $\Delta\eta \times \Delta\phi = 0.2 \times 0.2$ .

At Level 2, a cluster of energy in the calorimeter is identified as a “trigger electron” if (1) it is isolated and 90% of the energy is in the EM section of the calorimeter and (2) the shower shape is consistent with that expected for electrons.

W events are required to have one trigger electron with at least 20 GeV  $P_T$  and missing  $P_T$  of 20 GeV or more. The Z candidates are required to have two trigger electrons, each with  $P_T$  above 20 GeV.

In the offline reconstruction program, a cluster algorithm is used to find electron candidates and the calculation of the missing  $P_T$  is improved. After a candidate is identified as a cluster, selection criteria are applied to the candidate cluster to identify it as an electron. The candidate electron is required: (1) to have small hadronic leakage: EM fraction  $> 90\%$ ; (2) to have a shower shape consistent with that expected for electrons[5]; (3) to be isolated,  $[E(0.4 \text{ cone}) - EM(0.2 \text{ cone})]/EM(0.2 \text{ cone}) < 0.15$ ; (4) to have a track in the central detector that points to the cluster center; and (5) to be away from the intercryostat region and the module boundaries of the central calorimeter.

The W and Z event kinematics are further restricted offline. Table 1 summarizes the kinematic cuts used for W and Z events, and Table 2 gives the number of observed events categorized according to the location(s) of the decay electron(s) (In the table, CC is the central calorimeter,  $|\eta| \leq 1.1$ , ECN the north end calorimeter, and ECS the south end calorimeter.) In the following, we shall make use of only the W and Z events with electrons in the central calorimeter to determine the W mass.

### 3. Z mass measurement and EM energy scale

The well-measured Z mass at LEP serves as a useful calibration point. Two different

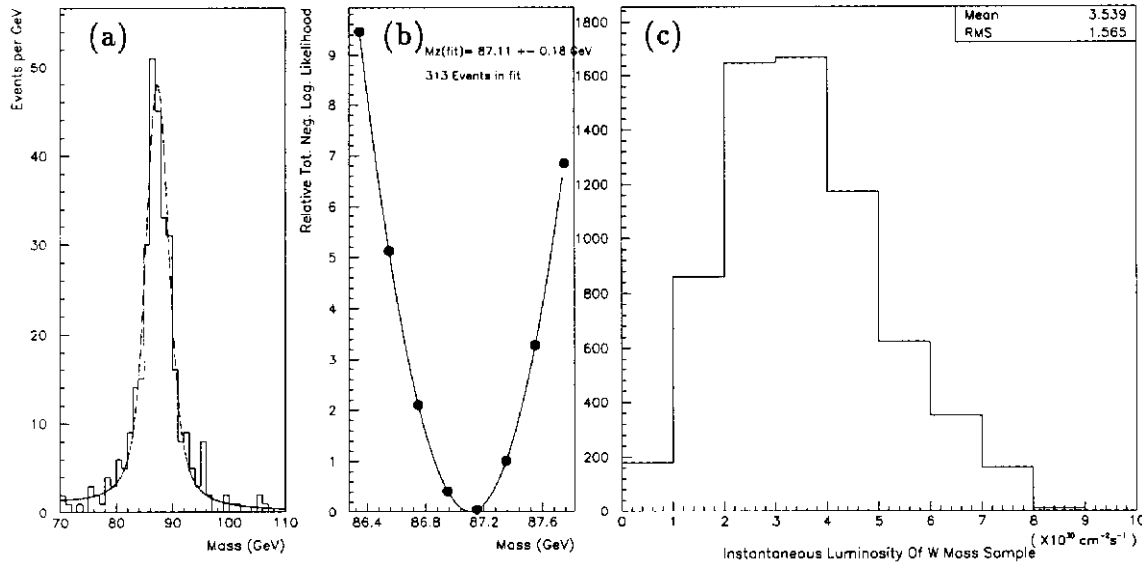


Figure 1: (a) The invariant mass of the two electrons with the best fitted curve superimposed. (b) The negative of the logarithm of the likelihood function (after moving the minimum to zero) as a function of the input Z mass. (c) The distribution in instantaneous luminosity of the W events used in the W mass measurement.

methods were used to measure the Z mass in the DØ experiment.

**Method I:** The ee invariant mass spectrum is modeled by a relativistic Breit-Wigner line shape with an exponential decay factor which accounts for the variation of the production cross section with mass. The detector response is taken into account by convoluting this distribution with a Gaussian response function on an event by event basis. Background is also taken into account. The likelihood function is calculated as a product over the 313 events in the sample and the negative of the logarithm of the likelihood function is minimized to determine the best fit to the data.

**Method II:** The second method starts by generating Z events in the same manner as W events (see section 4), again with a relativistic Breit-Wigner line shape. It then performs a fast detector simulation. The resulting Z invariant mass spectra are stored as function of the input Z masses, and compared with the data using a maximum likelihood method.

An extensive re-examination of the electromagnetic energy scale has been performed. The results are summarized in Table 3. In addition, a special EM trigger was used to study the uniformity of the central calorimeter. The trigger required an EM tower with  $P_T$  of 5 GeV or more at Level 1, and an EM cluster  $P_T$  of at least 7 GeV at Level 2. Some 3.5 million events were recorded. The data were used to provide a relative calibration of the CC modules. After incorporating all the corrections given in Table 3 and the relative calibration of the modules from the special study, the maximum likelihood analysis gives a Z mass of  $(87.11 \pm 0.18) \text{ GeV}$ . The fit to the data is shown in Fig. 1(a) and (b). The measured mass is four percent low when compared to the LEP Z mass.

Source of Correction	CC	ECN	ECS
Change HV 2.5kV $\rightarrow$ 2.0kV	+1.5 %	+1.6%	+1.6%
Test beam Pulser time dependence	-0.4%	-1.0%	-1.0%
Test beam beam momentum re-calibration	+0.5%	+0.1%	+0.1%
Optimization of sampling fraction	$\sim$ +2.0%	$\sim$ +2.0%	$\sim$ +2.0%
Algorithm difference (TB vs DØ)	0.1%	---	---
DØ calibration pulser instability	+0.5%	+0.5%	+0.5%
Liquid Argon temperature/purity	+1.0%	+1.2%	-1.2%
<i>Total Correction</i>	+5.2%	+4.4%	+2.0%

Table 3: Energy scale corrections (DØ Preliminary)

#### 4. Fast Monte Carlo simulation and comparison with data

The Monte Carlo simulation starts by generating a  $W$  event according to the spectrum in  $d^2\sigma/dP_T^W dy_W$  calculated by Arnold and Kauffman[6]. The  $W$  is then allowed to decay to an electron and a neutrino. After the  $W \rightarrow e\nu$  decay is generated, it is passed through a fast detector simulation. The electron  $P_T$ , the recoil of the  $W$ , and the underlying event from the spectator quarks in the  $\bar{p}p$  collision are modeled separately in the Monte Carlo.

The electron energy resolution is parameterized according to a formula that successfully describes measurements in the test beam,  $\sigma_e/E = \sqrt{c^2 + (s/\sqrt{E})^2 + (N/E)^2}$ , where the contributions from sampling fluctuations and calorimeter noise are obtained from test beam measurements,  $s = 0.14 \sqrt{\text{GeV}}$ , and  $N = 0.3 \text{ GeV}$ , and  $c$  is a constant obtained from a fit to the  $Z \rightarrow ee$  mass spectrum,  $c = (1.0 \pm 0.8)\%$ . The 0.8% uncertainty in the electron energy resolution contributes to the systematic error in the  $W$  mass.

The recoil of the  $W$ , with  $P_T^W$  and  $y_W$  obtained from the Arnold-Kauffman calculation, is treated as a jet and smeared according to the DØ jet energy resolution. The underlying event is modeled using real collider minimum bias events. Fig. 1(c) shows the distribution of instantaneous luminosity of the  $W$  events used for the  $W$  mass measurement. The spread is over a fairly large range of instantaneous luminosities. Minimum bias events for the underlying event are chosen at a scaled value of the luminosity that makes the multiple interaction rate in the Monte Carlo generated  $W$  events the same as in the  $W$  data sample. The similarity between a minimum bias event and the event underlying the  $W$  event is studied by looking at the scalar  $E_T$  as a function of pseudorapidity  $\eta$ . The disagreement is less than 10%. This uncertainty contributes to the uncertainty in the  $W$  mass and is included as a systematic error. The fluctuations in the underlying event and the uncertainty in the recoil momentum shift and smear the spectrum in transverse momentum of the  $W$ . These two effects cannot be separated in the data.

The scale in  $P_T^W$  relative to the EM scale is studied using  $Z$  events. In a  $Z$  event,  $P_T^Z$  can be obtained in two ways: from the measurement of the transverse momenta of the two electrons,  $\vec{P}_T^{ee}$ , and from the recoil activity in the  $Z$  event,  $-\vec{P}_T^{rec}$ , which is the way  $P_T^W$  is measured in  $W$  events. Fig. 2(a) shows a schematic view of the two measurements of the  $\vec{P}_T^Z$  projection onto the bi-sector of the angle between the electron  $\vec{P}_T$ 's, the  $\eta$  axis. The advantage of using the  $\eta$  axis is to minimize the effect of electron energy resolution. We

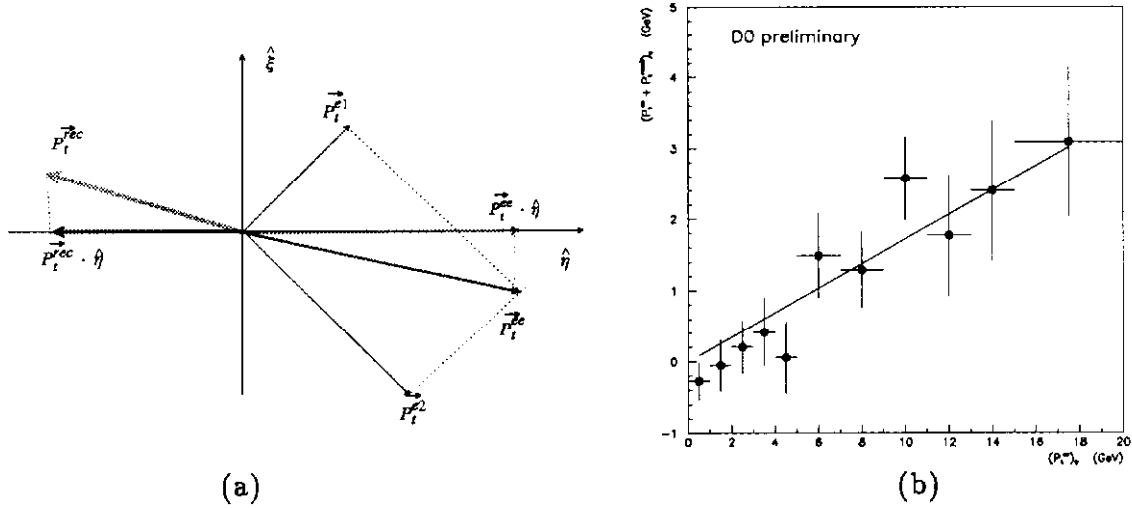


Figure 2: Projection of the EM and hadronic measurement of  $P_{tz}$  onto the bi-sector of the angle between the two electron  $P_T$ 's. (a) a schematic view. (b)  $\Delta$  vs  $\vec{P}_T^{ee} \cdot \hat{\eta}$ .

define the difference of the two measurements as:

$$\Delta \equiv \vec{P}_T^{ee} \cdot \hat{\eta} + \vec{P}_T^{rec} \cdot \hat{\eta} \quad (1)$$

A linear fit to  $\Delta$  as a function of  $\vec{P}_T^{ee} \cdot \hat{\eta}$  relates the hadronic recoil measurement of  $P_T^Z$  to that measured from the two electrons:  $P_T^{rec} = \alpha P_T^{ee}$ , see Fig 2(b). The value of  $\alpha$  found is  $0.83 \pm 0.06$ . The error has been expanded to include both the statistical error and deviations from linearity of the fit. The effect of this uncertainty on the W mass has been calculated and included as a systematic error.

Trigger efficiencies are modeled in the Monte Carlo simulation. The electron and missing  $P_T$  trigger efficiencies are studied independently as a function of offline electron and missing  $P_T$  respectively. These trigger turn-on curves are used in the Monte Carlo simulation. The trigger is 95% efficient for electrons with  $P_T = 25$  GeV and 90% efficient for missing  $P_T$  of 25 GeV.

A measure of the event selection biases— electron shape cuts, isolation cuts, etc.—can be obtained by studying the projection of the momentum recoiling against the W along the electron  $P_T$ , called  $u_{||}$  in Fig. 3(a). Electron selection criteria can bias the data against events in which the hadronic recoil against the W is large, and in the same direction as the electron. The projection  $u_{||}$  is plotted vs.  $P_T^W$  and compared to the Monte Carlo in Fig. 3(b).

Various calorimeter and tracking chamber fiducial cuts are also implemented in the Monte Carlo simulation.

## 5. Monte Carlo comparison with Data and Fitting Procedure

The W mass is extracted from the comparison between the experimental distribution and the Monte Carlo simulation. In principle, electron  $P_T$ , missing  $P_T$  and transverse mass can

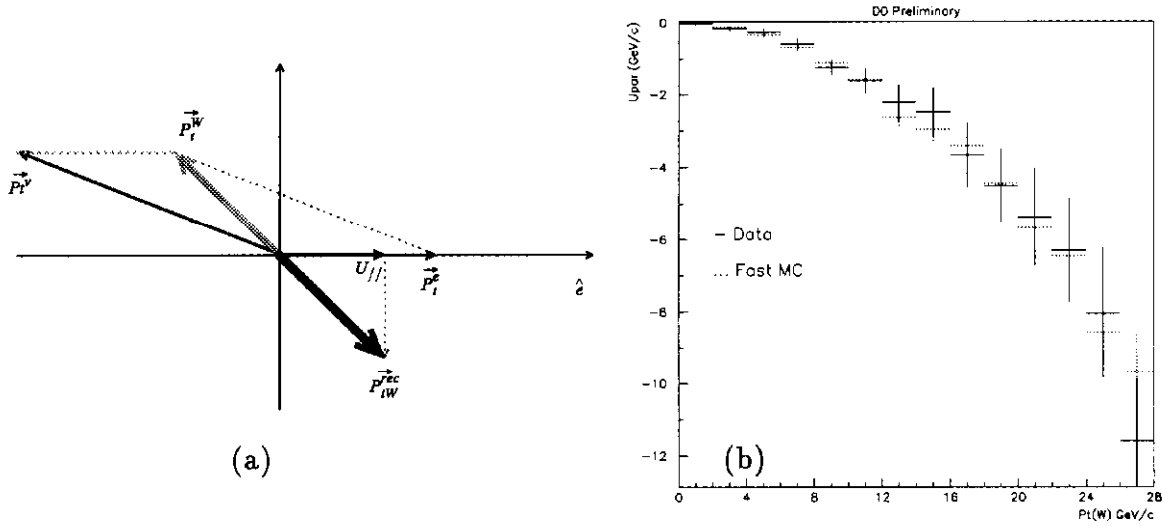


Figure 3: (a) Definition of  $u_{||}$ . (b)  $u_{||}$  vs  $P_T^W$ .

all be used to extract the W mass.

The transverse mass is defined in the plane transverse to the  $\bar{p}p$  beam in a manner analogous to the definition of the invariant mass.

$$m_T^2(W) = (P_T^e + P_T^\nu)^2 - (\vec{P}_T^e + \vec{P}_T^\nu)^2 \quad (2)$$

$$= 2P_T^e P_T^\nu (1 - \cos \phi_{e\nu}) \quad (3)$$

where  $P_T^e$  and  $P_T^\nu$  are the electron and neutrino transverse momenta, and  $\phi_{e\nu}$  is the angle between the electron and the neutrino in the transverse plane. The neutrino  $P_T$  comes from the missing  $P_T$  measurement, which involves all the calorimeter cells. It generally suffers from poor resolution and detector biases. Among the three quantities, the electron  $P_T$  is the best measured. But W's are not produced at rest. The transverse momentum of the electron is sensitive to  $P_T^W$ . The spectrum in  $P_T^W$  can be modeled theoretically but only with large uncertainty. On the other hand, transverse motion of the W shifts the transverse mass only by terms of order  $P_T^{2W}/(m_W^2 + P_W^2)$ [7]. Generally, smaller systematic errors are expected fitting the transverse mass distribution than fitting either the electron or neutrino  $P_T$  distributions. The electron and neutrino  $P_T$  distributions serve as good cross checks.

The fast simulation generates transverse mass spectra as a function of the input W mass. These spectra are compared with data using a maximum likelihood method. Fig. 4(a) shows the best fit Monte Carlo transverse mass spectrum overlapped with the data.

Fig. 4(b), and Figs. 5(a), (b), (c), and (d) show the comparison between data and Monte Carlo for the spectra in W, electron, and neutrino transverse momenta, and also for the distributions in the variables  $u_{||}$  and  $u_{\perp}$ . In these comparisons, the W mass obtained from the fit to the transverse mass was used in the Monte Carlo simulation. Data and Monte Carlo agree very well. The W mass is obtained from a fit with a fixed W width of 2.12 GeV. The W mass scaled by the ratio of the Z mass measured at LEP to the Z mass measured in

D0 Preliminary:  $W \rightarrow e \nu$  Decays(CC only)

D0 Preliminary:  $W \rightarrow e \nu$  Decays(CC only)

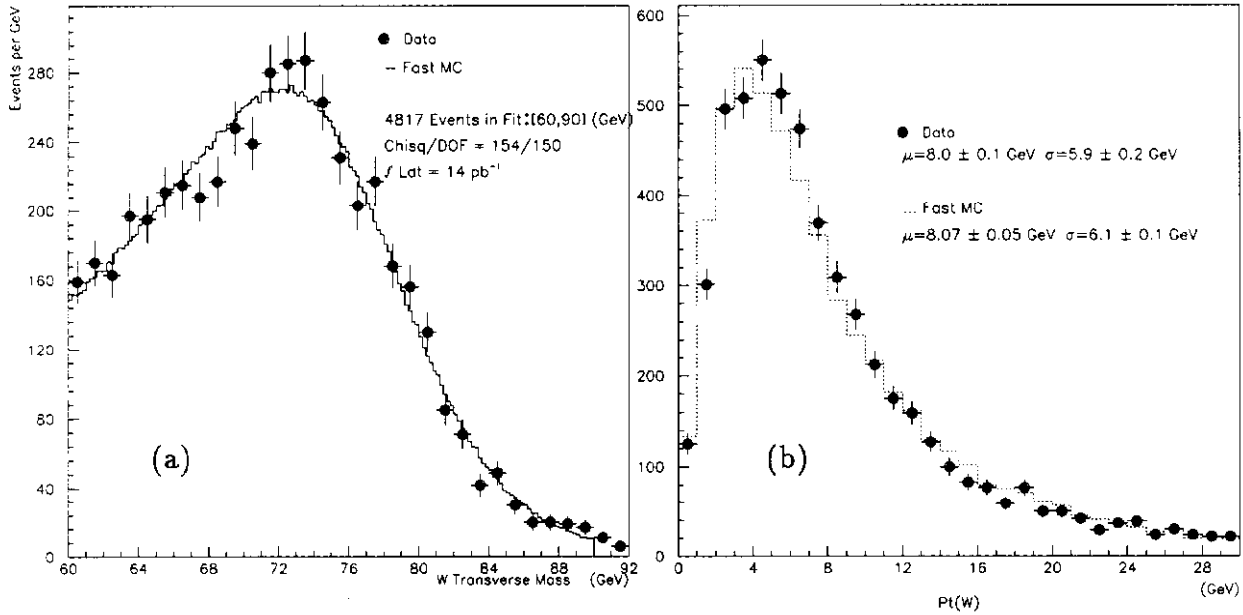


Figure 4: (a) Transverse mass spectrum compared to Monte Carlo simulation. The chi-squared was calculated by comparing data and Monte Carlo in 200 MeV bins in transverse mass between 60 GeV and 90 GeV. (b) Spectrum in  $P_T^W$  compared to the Monte Carlo simulation.

D0 Preliminary:  $W \rightarrow e \nu$  Decays(CC only)

D0 Preliminary:  $W \rightarrow e \nu$  Decays(CC only)

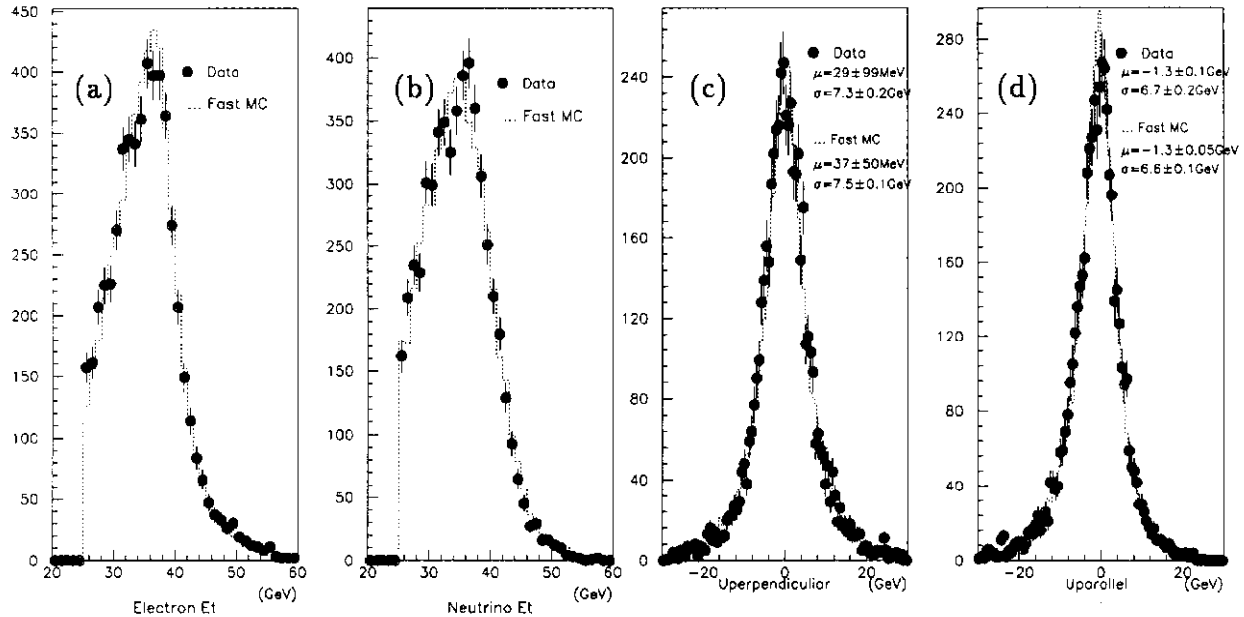


Figure 5: The overlap of Monte Carlo simulation (curve) onto data distribution (dots with error bars). (a) Electron  $P_T$ . (b) neutrino  $P_T$ . (c)  $u_{\perp}$ . (d)  $u_{\parallel}$ .

Source of Uncertainty	MeV
Trigger Efficiency	20
Resolution and neutrino $P_T$ scale <sup>†</sup>	149
Energy underlying electron	50
$u_{  }$ efficiency	10
Hadronic to EM scale	80
QCD background	30
Theoretical model uncertainty <sup>‡</sup>	86
W width	20
Fitting Error	30
<i>Total</i>	200

† Resolution and neutrino $P_T$ scale	
Electron energy resolution	70
Neutrino $P_T$ scale, resolution (W underlying event)	130
Jet energy resolution	20
.	
.	
‡ Theoretical model uncertainty	
Structure function	70
$P_T^W$ spectrum	50

Table 4: Systematic uncertainties on the W mass measurement(DØ Preliminary)

this experiment, is

$$M_w = (79.86 \pm 0.16(stat)) GeV \quad (4)$$

## 6. Systematic, Scale Errors

Table 4 shows the various contributions to the systematic errors. The total systematic error is 200 MeV. The effect of radiative decays is still under study.

Two methods are used to determine the energy scale error.

- **Method I** : Uses both Z and  $J/\psi$  signals to constrain the EM scale.
- **Method II**: Uses Z events alone to obtain the EM scale and offset.

**Method I:** We have observed  $J/\psi \rightarrow e^+e^-$  with more than  $3\sigma$  significance. Fig. 6(a) shows the ee invariant mass spectrum in the region of the  $J/\psi$ . The measured mass is  $m_{J/\psi} = (3.00 \pm 0.27) GeV$ .

We define the scale factor  $\alpha$  and energy offset  $\beta$  through the following formula:

$$E_{true} = \alpha E_{measured} + \beta \quad (5)$$

where  $E_{true}$  stands for the true electron energy and  $E_{measured}$  is the electron energy measured in the calorimeter. The invariant mass of the two electrons is:

$$m_{true} = \sqrt{2E_1^{true} E_2^{true} (1 - \cos \gamma)} \quad (6)$$

where  $\gamma$  is the opening angle between the two electrons. Substituting Eq. 5 into Eq 6, we have

$$m_{true} \simeq \alpha m_{measured} + \beta f \quad (7)$$

where  $f = 2(E_1^{measured} + E_2^{measured})/m_{measured} \sin^2(\gamma/2)$ . Using the measured Z and  $J/\psi$  masses, and the average f-factors for the two decays, we find  $\alpha = 1.047 \pm 0.009$ ,  $\beta =$

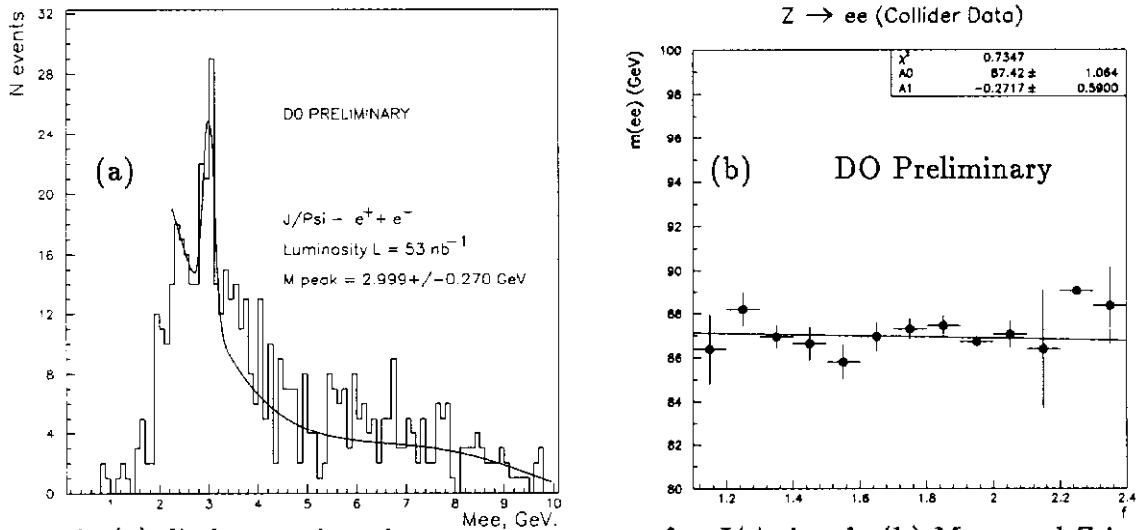


Figure 6: (a) di-electron invariant mass spectrum for  $J/\psi$  signal. (b) Measured Z invariant mass as a function of the f-factor with fitted curve.

$12 \pm 340$  MeV. The parameters  $\alpha$  and  $\beta$  are strongly correlated, as one might expect. The corresponding error in the W mass is  $\delta(M_W) = 195$  MeV.

**Method II:** Electrons from Z decays are not monochromatic. Electrons in the central calorimeter vary in energy from 45 GeV to 70 GeV. For Z decays with electrons back to back, i.e.  $E_1 \simeq E_2 \simeq 45$  GeV, the f factor is about 2. For Z decays with small opening angles, i.e.  $E_1 \simeq E_2 \simeq 70$  GeV, the f-factor is about 1.5. A linear fit to the measured Z mass as a function of the f-factor is shown in Fig. 6(b), and gives  $\alpha = 1.043 \pm 0.013$ ,  $\beta = 270 \pm 620$  MeV. These values are consistent with those determined from the first method. Again,  $\alpha$  and  $\beta$  are strongly correlated. The advantage of this method is that it fixes the electron energy scale using high energy electrons in the same energy range as those from W decays. With this method we arrive at a scale error of  $\delta(M_W) = 310$  MeV.

## 7. Consistency Checks

**Varying the Fitting Window :** Transverse masses between 60 and 90 GeV were fit to obtain the W mass. Using instead minimum transverse masses of 50 GeV and 70 GeV changes the W mass by 50 MeV and 140 MeV respectively. To separate the statistical contribution from any real shift due to Monte Carlo biases, we repeated this exercise with 40 Monte Carlo samples. Each has the same statistics as the data. We found that the 40 samples give a mean shift of 30 MeV with a rms deviation of 140 MeV. The 30 MeV shift is used as the systematic error in the fitting method.

We also varied the upper transverse mass cut to 92 and 94 GeV. The change in the W mass is 20 MeV in each case. The same exercise on 40 Monte Carlo samples gives a mean shift of 10 MeV with a rms deviation of 20 MeV.

**Select single vertex W events:** We restricted the sample to include only events with one vertex. This reduced the event sample by 23%. The W mass from this sample is  $79.84 \pm 0.18$  GeV.

**Tightening the electron selection cuts:** Tighter cuts were imposed on the electron,

requiring that there be only one track in the electron finding road and that the ionization in the central tracking system be less than twice that from a minimum ionizing particle. The event sample is reduced by 22%. An independent study indicates that the QCD background is reduced by a factor of two. The fit to this sample gives  $M_W = (79.89 \pm 0.18) \text{ GeV}$ . This result is consistent with the  $(2 \pm 1)\%$  QCD background in the W sample obtained from an independent study.

## 8. Summary and Prospects

We have made a preliminary measurement of the W mass using electrons in the central calorimeter,  $|\eta| \leq 1.1$ . Using the conservative approach of method II to fix the energy scale, our measured W mass is:

$$M_W = 79.86 \pm 0.16(stat) \pm 0.20(syst) \pm 0.31(scale) \text{ GeV} \quad (8)$$

As the analysis progresses, we expect to reduce both scale and systematic errors. Work is in progress to incorporate data at larger  $|\eta|$ .

In Tevatron Run 1(b), scheduled to begin at the end of this year, we expect to quadruple the data, reducing further the statistical error, as well as the scale and systematic errors, which are largely tied to the number of Z events.

## References

- [1] R. Tanaka, talk given at the *XXVI Int. Conf. on High Energy physics*, Dallas, Texas, August, 1992.
- [2] S. Fanchiotti, B. Kniehl, and A. Sirlin, *Incorporation of QCD Effects in Basic Corrections of the Electroweak Theory*, CERN-TH-674992, NYU-TH-921205.
- [3] A. Sirlin, *Radiative corrections in  $SU(2)_L \times U(1)$  theory : A simple renormalization framework*, Phys. Rev. D22, 971 (1980).
- [4] W. J. Marciano and Z. Parsa, Snowmass 1982, p.155.
- [5] M. Narain, *Electron identification in the  $D\bar{O}$  Detector*, *Proceeding of the 7th Meeting of the American Physical Society Division of Particle and Fields*, Nov. 10-14, 1992, p.1678.
- [6] P. Arnold and R.P. Kauffman, *W and Z production at next-to-leading order: from large  $q_T$  to small*, ANL-HEP-PR-90-70.
- [7] J. Smith, W. L. van Neerven, and J. A. M. Vermaseren, *Transverse mass and width of the W boson*, ITP-SB-83-11; Phys. Rev. Lett. 50:1738 (1983).